

# Super-Toughed Polymer Blends Derived from Polypropylene Random Copolymer and Ethylene/Styrene Interpolymer

Jian Tang,<sup>1,2</sup> Weihua Tang,<sup>1,2</sup> Huilin Yuan,<sup>2</sup> Riguang Jin<sup>2</sup>

<sup>1</sup>College of Chemical Engineering, Nanjing University of Science and Technology, Nanjing 210094, People's Republic of China

<sup>2</sup>School of Materials Science and Engineering, Beijing University of Chemical Technology, Beijing 100029, People's Republic of China

Received 17 September 2008; accepted 29 June 2009

DOI 10.1002/app.31035

Published online 27 August 2009 in Wiley InterScience (www.interscience.wiley.com).

**ABSTRACT:** In this article, blends of polypropylene random copolymer (PP-R) with a novel impact modifier, namely ethylene/styrene interpolymer (ESI), were prepared to evaluate the effectiveness of ESI in toughening PP-R and the influence of ESI content on the mechanical, thermal, and rheological properties of polymer blends. Results showed that super-toughened PP-R/ESI blends (ca. Izod impact strength  $\geq 500$  J/m) were readily achieved with only 5 wt % ESI. The blends exhibited significant improvement in both impact strength and elongation, while small loss in tensile strength and elastic modulus

when increasing ESI content. ESI had a nucleating effect that caused PP matrix to crystallize at higher temperatures, whereas PP-R/ESI blends presented lower melting temperatures ( $T_m$ ) than PP-R matrix and  $T_m$  decreased with the increment of ESI content. Rheology study indicated that both PP-R matrix and PP-R/ESI blends presented shear thinning behaviors during melt processing. © 2009 Wiley Periodicals, Inc. *J Appl Polym Sci* 115: 190–197, 2010

**Key words:** polypropylene random copolymer; ethylene/styrene interpolymer; super-toughened polymer blends

## INTRODUCTION

Polypropylene (PP) is one of the most widely used plastics, featuring good mechanical and thermal properties, chemical resistance, and easy processability.<sup>1</sup> However, PP's engineering applications are often limited by its fracture toughness at low temperature and in particular its high notch sensitivity at room temperature. Great efforts have been made in the toughening of PP over the last two decades.<sup>2</sup> An effective approach is to blend PP with rubber-type impact modifier, such as ethylene-propylene copolymer,<sup>3–6</sup> ethylene-propylene diene monomer,<sup>7–10</sup> ethylene vinyl acetate,<sup>11–14</sup> styrene-*b*-butadiene-*b*-styrene (SBS), styrene-*b*-hydrogenated butadiene-*b*-styrene triblock copolymers (SEBS),<sup>14</sup> and ethylene-1-octene copolymer (POE).<sup>15–18</sup> These rubber-toughened PP blends generally achieve significant improvement in both toughness (i.e., impact strength) and ductility (i.e., elongation at break), while suffer from a great loss in stiffness (i.e., elastic modulus and tensile strength). The toughening efficiency is highly dependent on the

content, particle size, architecture of rubber, and the interactions between phases determining the mechanical properties of the polymer blends.<sup>19–24</sup>

The incorporation of a rubbery phase in PP can also be achieved by copolymerization propylene with small proportion of ethylene in the polymerization process,<sup>25</sup> a new type of PP, namely, polypropylene random copolymer (PP-R) is synthesized and features long propylene sequences and occasional ethylene units along its polymer backbone. PP-R displays excellent thermal stability, aging resistance, and mechanical properties, making it attractive for piping systems for both domestic and industrial applications.<sup>26–31</sup> However, PP-R still suffer from low impact-resistance in applications like PP, especially at low service temperatures.<sup>29,30</sup> Surprisingly, only limited researches have addressed this issue so far. Forte and coworkers<sup>32</sup> recently reported their toughening study of PP-R with SBS and SEBS. They found SEBS is a more efficient impact modifier for PP-R than SBS and both act as nucleating agent for matrix crystallization. It was explained that EB segments in SEBS caused PS disperse better in PP matrix, thus smaller rubbery domains formed with lower coalescence levels.<sup>32</sup>

In this article, we report our efforts to achieve super-toughened PP-R blends by using ethylene/styrene interpolymer (ESI) as impact modifier. ESI are a

Correspondence to: W. Tang (tang-wh@hotmail.com) or H. Yuan (yuanhuil@263.net).

series of new polymers developed by Dow Chemical Company using INSITE™ technology.<sup>33–35</sup> The ESIs have substantially random incorporation of styrene except successive head-to-tail styrene chain insertions.<sup>36</sup> This feature differentiates interpolymers from truly random copolymers of ethylene and styrene.<sup>37</sup> Thus, regarding chain flexibility and entanglement network, ESIs provide an unusual opportunity to approach the amorphous state of polyethylene without the constraints of the inevitable crystallinity.<sup>38</sup> ESIs show excellent compatibility and good toughening effect to styrenic polymers, polyolefins, and a wide variety of other thermoplastics due to their inherent combination of olefinic and styrenic functionality in the backbone of polymer chains.<sup>39</sup> In our previous work, ESI ( $M_w = 240,000$ , 29.3 wt % PS content) showed good compatibilization effect toward polyethylene (including HDPE and LDPE) and polystyrene.<sup>40,41</sup> The possible consequences of blending ESI with compatible PP-R are very intriguing to us and thus motivated this study.

The objective of this study is to evaluate simultaneously the effectiveness of ESI as an impact modifier and the influence of ESI content on the mechanical and thermal properties of PP-R/ESI blends. In addition, the rheological properties of PP-R and PP-R/ESI blends are also studied, aiming to provide some insight on processability of PP-R and its blends.

## EXPERIMENTAL

### Materials

PP-R (C4420, 3 wt % ethylene) with 0.3 g/10 min melt flow index (MFI) (at 230°C under 2.16 kg load) was supplied by Yanshan Petrochemical Co. (Beijing, China). ESI (ESI24,  $M_w = 240,000$ , 29.3 wt % PS) was provided by Phil Island Co. (Houston, TX).<sup>33–35,40,41</sup>

### Preparation of polymer blends

The components of PP-R/ESI blends were dried at 80°C overnight in a vacuum oven and physically mixed according to formulations. Polymer blends were extruded using a corotating twin-screw extruder (SLF-35B, L/D = 30, Keqiang Polymer Engineering Company, Chengdu, Sichuan, China) with a rotation speed of 200 rpm. The barrel temperature profile was 180/200/220/230/230/210°C, where the latter refers to the die temperature. The extruded materials were injection-molded into standard dumbbell tensile bars and notched impact specimens using an injection-molding machine (SZ-160/80 NB, China). The cylinder temperature and molding temperature during molding injection were 200 and 80°C, respectively.

### Characterization of mechanical properties

The tensile tests were carried out on an Instron tensile tester (model 3211) according to ASTM D638 with a crosshead speed of 10 mm/min. The notched Izod impact tests were performed on a pendulum impact testing machine (XJ-40A, Wuzhong Material Testing Machine Company, Hebei, China) according to ASTM D256. Five specimens of each formulation were tested, and the average values were reported. All tests were performed at 23°C.

### Microscopy

The morphology of the blends was examined using a Cambridge-S250 scanning electron microscope (SEM). The samples of PP-R/ESI blends were cryogenically fractured in liquid nitrogen, and ESI phase in the fractured surface was etched with tetrahydrofuran (THF) at 50°C for 1 h. The samples were dried and sputter-coated with a thin layer of gold before examination. In addition, fractured surfaces of PP-R/ESI blends near the notch were directly sputter-coated a thin layer of gold and used for SEM studies.

### Thermal analysis

The thermal behavior of PP-R matrix and PP-R/ESI blends was analyzed using Perkin-Elmer Differential Scanning Calorimeter (model DSC Pyris 1) at nitrogen atmosphere. Samples were heated to 200°C, held for 3 min at the same temperature, and then cooled down to room temperature at 10°C/min. They were reheated to 200°C at the same heating rate. Crystallization and melting temperatures ( $T_c$  and  $T_m$ ), and fusion enthalpy ( $\Delta H_m$ ) were taken from the second and third run curves, respectively. Sample crystallinity was calculated by taking PP fusion enthalpy 190 J/g as the reference value.<sup>32</sup>

### Rheological measurement

To gain the insight of the processability of PP-R, its rheological behavior was specifically studied using an in-line extrusion rheometer, mounted at the exit end of the single-screw extruder (PLD-651, L/D = 25, BRABENDER). The measurement of melt viscosity was conducted on the basis of polymer melt flow through a vertically tapered slit, which reflects on the pressure drop and the flow rate of polymer melt through the wedge.<sup>42</sup> Two pressure transducers (Dynisco Model TPT 4636) were installed in the rheometer to measure the pressure drops. This unique rheological properties characterization vividly simulates the practical processing scenario of PP-R. For polymer blends, their rheological properties were evaluated as usual using an Instron

capillary rheometer (capillary diameter 1.262 mm,  $L/D = 60.51$ ) at 200°C. The experiments are carried out at 200°C under the shear rates varying from 1 to  $10^4 \text{ s}^{-1}$ .

## RESULTS AND DISCUSSION

### Mechanical properties

PP-R/ESI polymer blends were melt-blended according to the weight ratio 95/5, 90/10, 85/15, 80/20, 75/25, 70/30, and 65/35. The results of Izod impact strength, tensile strength, elongation at break, and elastic modulus for PP-R/modifier blends are summarized in Table I. With the addition of modifier, the impact strength of the blends is significantly improved. As shown in Table I, a three-time increase in impact strength was observed from PP-R/ESI blend with 5% addition of ESI. In all cases, super-toughened PP-R/ESI blends (notched Izod impact strength  $> 500 \text{ J/m}$ ) are obtained with no less than 5 wt % of ESI content. Nearly 4.5-fold increment in impact strength of PP-R (from 180 to 838  $\text{J/m}$ ) is achieved with 20 wt % ESI addition. Since ESI has ethylene segments (content, 70 wt %) in its polymer chains, these flexible polyethylene blocks in ESI have higher affinity or compatibility with PP matrix. This affinity will cause PS block to disperse better in PP matrix in melt state. An examination on glass transition temperature of ESI ( $T_g \sim 0^\circ\text{C}$ )<sup>35</sup> and PP matrix ( $T_g \sim -15^\circ\text{C}$ )<sup>32</sup> one can find that ESI domains are slightly rigid in comparison with PP-R matrix. When PS blocks well disperse in PP-R matrix, ESI domains, just like most rubbers, may act as stress concentrators and absorb more impact energy by deformation during external impact. Increasing ESI content will contribute to significant improvement in toughness for PP-R matrix. Most ESI droplets dispersed in PP-R matrix with a domain size around 1–3  $\mu\text{m}$  when ESI content approaches 20 wt % (refer to SEM images in Fig.

**TABLE I**  
Izod Impact Strength, Tensile Strength, Elongation at Break and Elastic Modulus of PP-R/ESI Blends at 23°C

PP-R/ESI	Izod impact strength (J/m)	Tensile strength (MPa)	Elongation at break (%)	Elastic modulus (MPa)
100/0	180	28.7	422	354.3
0/100 <sup>a</sup>	n/a	33.3	517	26.3
95/5	546.7	27.8	681	305.9
90/10	685	26.7	749	293.4
85/15	751.2	25.6	892	273.1
80/20	838.3	25.3	919	271.4
75/25	926.4	25.0	1147	268.7
70/30	1012.6	24.8	1244	256.5
65/35	1103.2	24.4	nb	254.2

<sup>a</sup> Data are obtained from Ref. 34 n/a: not available; nb: no break.

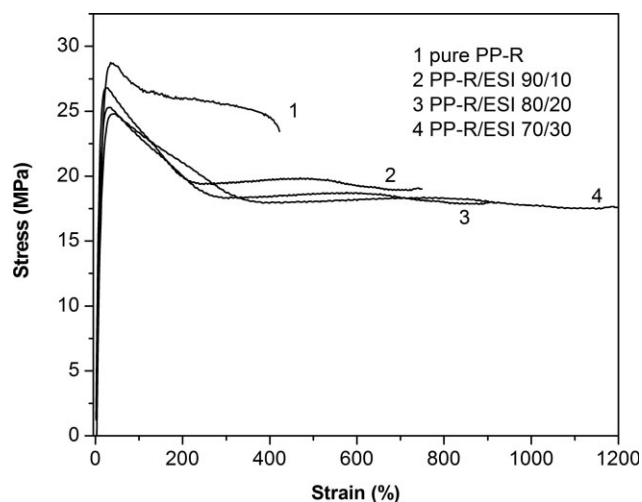


**Figure 1** Stress-strain curves of pure PP-R and PP-R/ESI blends with varied concentration of ESI.

2). The differences in Young's modulus and Poisson's ratio between ESI droplets and PP-R matrix induced compressive stress onto the more finely dispersed ESI domains. Consequently, the deformation mechanism in dispersed particles may change from crazing to cold drawing, and thus absorbed more external impact. Interestingly, the rate of impact strength development decreases considerably with ESI addition. This behavior may be explained by blend morphology. As we know, with the addition of ESI, more stress concentrators are formed to absorb more energy, while ESI droplets increase in their domain sizes. After their domain sizes overpass the optimum size for toughening efficiency, the rate of toughness development with ESI content slows down.

A close look at the stress-strain curves (Fig. 1) of neat PP-R and PP-R/ESI blends, the typical ductile plastic fracture behavior with a yield stress and following large strain is observed in all curves. However, the incorporation of ESI significantly changed the nature of the curves. With the addition of ESI, the yield stress of PP-R/ESI blends gradually decreases, whereas the strain increases dramatically. This behavior can also be attributed to the good affinity of ethylene segments with PP matrix. The reduction in yield stress and increase in strain with increasing modifier content is similarly observed in PP-R/SEBS and PP-R/SBS blends.<sup>32</sup> For the ductility of PP-R blends, it is noted that the PP-R/ESI blends showed greater deformation and did not break even at over 300% elongation with 35 wt % ESI.

As for stiffness of the polymer blends, the addition of modifier brings certain loss in the tensile strength and elastic modulus. However, due to the existence of ESI, PP-R/ESI blends suffer from slow decrease in both tensile strength and elastic modulus. Careful inspection of the tensile strength and

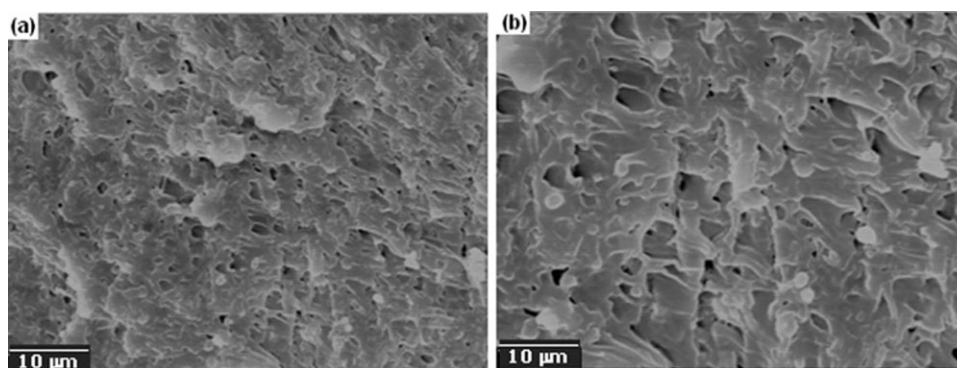


**Figure 2** SEM micrographs of cryogenically fractured and THF-etched surfaces for (a) PP-R/ESI 90/10 blend, and (b) PP-R/ESI 80/20 blend.

elastic modulus data, one can find the former only dropped 12% and the latter lost 23% when 20 wt % ESI was added. But PP-R/ESI 20 wt % harvested over three-fold increase in impact strength and one-fold increase in elongation.

Taking into account of toughness, ductility and stiffness of PP-R blends, the addition of ESI brings significant improvement in toughness and ductility while slow decrease in stiffness for PP-R-ESI blends. Overall, ESI-toughened PP-R blends exhibit higher mechanical properties due to the particular ESI structure.

### Fractography

The brittle-ductile transition (BDT) of rubber-toughened PP and nylon blends was studied by optimizing processing temperature when blends were made<sup>9,10</sup> and strain rate applied in mechanical property characterization.<sup>43</sup> Shear yielding of matrix was proposed to be responsible for the rubber toughening of semicrystalline polymers like PP and nylon. Impact and high speed tensile test of PP/POE blends showed that notched impact deformation was actually high speed tensile deformation near notch tip.<sup>43</sup> To reveal the higher efficiency of ESI in toughening PP-R, we investigated PP-R deformation

by observing the fracture surfaces and the impact-fractured surface near notch tip of PP-R/ESI.

As shown in the SEM micrographs (Fig. 2), after extracting ESI phase with THF, numerous voids were observed in the rough fracture surfaces. The surfaces presented typical droplet-matrix morphology for PP-R/ESI blends. The droplets of impact modifier are well dispersed in PP-R matrix. When subjected to external forces, ESI domains act as stress concentrators to absorb external impact force. When comparing the domain size in PP-R/ESI 10 wt % [Fig. 2(a)] with that in PP-R/ESI 20 wt % [Fig. 2(b)], ESI droplets were smaller in the former, accompanying with lower droplet coalescence levels. The coalescence of several small ESI droplets formed larger unevenly shaped rubbery domains in PP matrix for PP-R/ESI 20 wt % blends [Fig. 2(b)]. The diameters of ESI droplets range from 1 to 3  $\mu\text{m}$ , whereas the coalescence ESI domain sizes range from 3 to 6  $\mu\text{m}$ . The average diameter of elastomer particle size increased for higher SBS content, attributed to elastomer particles coalescence, was also observed by Felisberti in PP/SBS blends.<sup>44</sup>

When directly picturing the impact-fractured surfaces of PP-R/ESI blends, one can observe a typical SEM micrograph as shown in Figure 3(a), which displays two regions: slow growth region initiated at the notch root, indicated as void zone [Fig. 3(b)] and

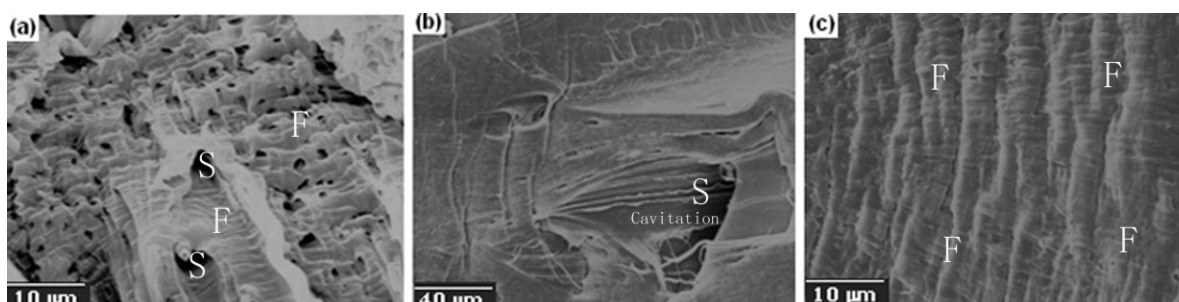


**Figure 3** SEM micrographs of notch tip of the impact-fractured surface of PP-R/ESI 95/5, (a) overview, (b) detailed cavitation feature (slow growth region), and (c) detailed fibrillar feature (fast growth region).

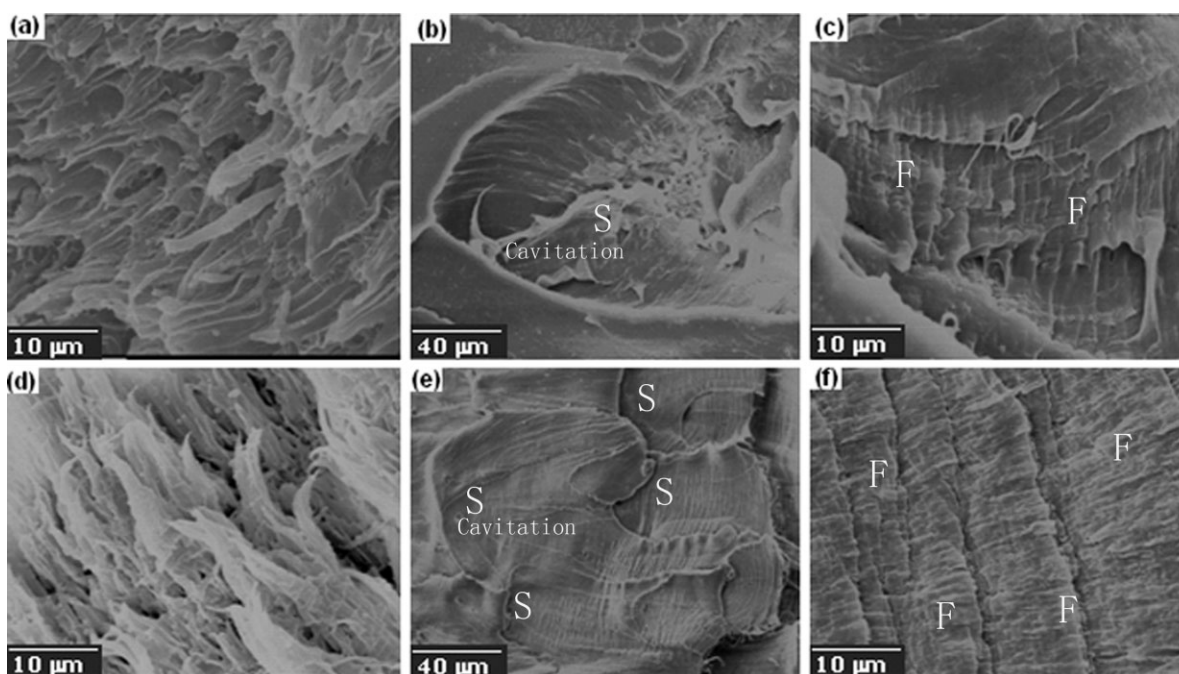


**Figure 4** SEM micrographs of notch tip of the impact-fractured surface of (a) overview of PP-R/ESI 85/15 and (d) overview of PP-R/ESI 70/30 blends, with detailed cavitation features (slow growth region) shown in (b, e), and detailed fibrillar features (fast growth region) shown in (c, f).

the subsequent fast crack growth region, indicated as fibrillar zone [Fig. 3(c)]. The void zone exhibits a smooth and annular-layered surface [Fig. 3(b)], while fast growth region is composed of coarse nonplanar lamella [Fig. 3(c)]. Cavitations are clearly seen in the slow growth region adjacent to the notch root, which is thought to be largely responsible for the enhancement of impact strength of the blends. These cavitations were observed when ESI domains were deformed after impact tests. As mentioned above, ESI domains act as stress concentrators, which absorb the impact deformation energy to produce BDT in addition to shear yielding of crazing of matrix. Cavitations occurring in just small area near to the notch root were also observed in poly(ethylene terephthalate) (PET) toughening blends with a maleic anhydride grafted styrene ethylene/butylene-styrene triblock copolymer (SEBS-*g*-MA).<sup>45</sup> In these PET/SEBS-*g*-MA blends, the impact-fractured SEM micrographs also presented two regions: one for slow growth initiated at the notch root followed by another for subsequent fast crack growth.

When increasing of ESI concentration [Fig. 4(a,d)], more annular-layered cavitations with decreased diameter are initiated in the slow growth regions [Fig. 4(b,e)]. The diameter of these cavitations fall in the range of 50–100  $\mu\text{m}$ , which is much less than the width of notch for the impact specimens. According to the theoretical calculation by Yang et al.,<sup>43</sup> the strain rate of the narrow notch can be high as 6000/s at the beginning of impact tests. Therefore, this

notched impact deformation is actually a high speed tensile deformation near the notch tip. SEM images in fast growth regions [Fig. 4(c,f)] shows the shear yielding matrix surfaces exhibited corrugated lamella structure. The more cavitations initiated, the more impact energy was absorbed by the polymer blends can absorb, which is displayed in mechanical properties as dramatic increase in impact toughness, and the matrix resin is transferred from ductile materials into high ductile materials or even super-toughened materials. It is noted that 5.6-fold enhancement in impact strength of PP-R is achieved with the addition of 30 wt % ESI. The fracture behavior of PP-R/ESI blends is very similar to that observed in PET/SEBS-*g*-MA.<sup>45</sup>

#### Thermal behavior

As discussed above, the addition of ESI leads to super-toughened PP-R blends. To correlate the improved toughness with crystallinity of PP-R matrix, thermal behavior of PP-R and PP-R/ESI blends was evaluated with DSC measurements. The crystallization temperatures of exothermic DSC curves of pure PP-R and PP-R/ESI are shown in Figure 5. Compared with pure PP-R, the crystallization peaks of all polymer blends were displaced to higher temperatures, which demonstrates ESI act as a nucleation agent for PP-R. The highest crystallization temperature ( $T_c$ ), measured as the apex of the crystallization peak, was found in PP-R/ESI (95/5) blend. Further increasing the concentration of ESI,

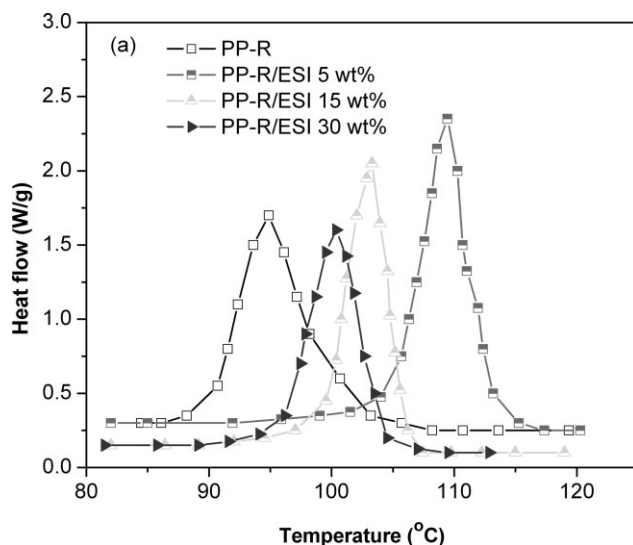


**Figure 5** Crystallization peak of exothermic DSC curve of pure PP-R and PP-R/ESI blends.

polymer blends present exothermic peaks falling between that of PP-R and that of PP-R/ESI (95/5) blend. All crystallization peaks of PP-R blends are slightly narrower than that of pure PP-R, which indicates that PP-R/ESI blends have narrower distribution in crystallite sizes. Such displacement in crystallization peaks was also observed in PP-R/SBS and PP-R/SEBS blend systems.<sup>32</sup>

Table II summarizes the  $T_m$ ,  $T_c$ ,  $\Delta H_m$ , and crystallinity values for all PP-R/ESI blends. Our PP-R shows lower melting temperature (143°C) than i-PP (163°C) due to the ethylene insertion in the PP chain, which disrupts the isotactic sequences, decreases the size of lamella and introduced defects in the crystallite.<sup>46</sup> In general, PP-R blends present lower  $T_m$  than pure PP-R. For the fusion enthalpy, there is an increase in  $\Delta H_m$  up to 15 wt % ESI. At higher modifier content (>15 wt %), the blends exhibit lower  $\Delta H_m$  than PP-R. The matrix crystallinity results listed in Table II show ESI caused PP-R crystallinity to increase, which contributes to an improved mechanical properties of the polymer blends in terms of toughness.

**TABLE II**  
Melting ( $T_m$ ) and Crystallization ( $T_c$ ) temperatures, Fusion Enthalpy ( $\Delta H_m$ ) and Crystallinity of PP-R/ESI Blends

PP-R/ESI	$T_c$ (°C)	$T_m$ (°C)	$\Delta H_m$ (J/g)	Crystallinity (wt %)
100/0	94.9	142.9	68.6	36
95/5	109.4	142.8	77.8	43
90/10	103.3	141.9	71.2	42
85/15	102.9	140.9	66.6	41
80/20	101.6	140.6	62.3	41
70/30	100.4	140.2	53.2	40

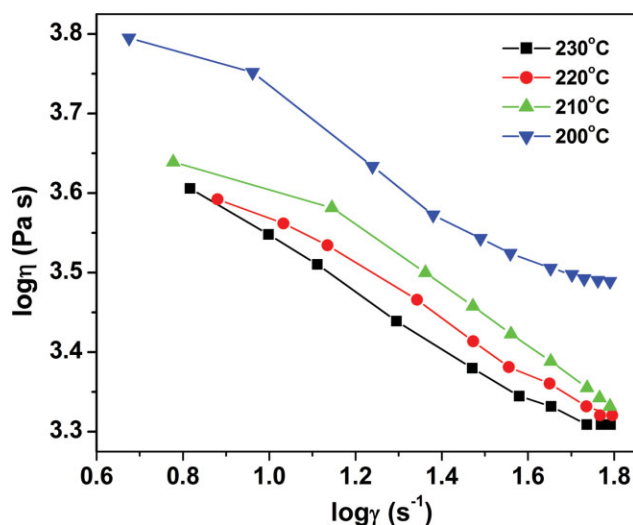


**Figure 6** Shear thinning of the PP-R apparent viscosity behavior at varied temperatures. [Color figure can be viewed in the online issue, which is available at [www.interscience.wiley.com](http://www.interscience.wiley.com).]

## Rheology

The rheological properties of polymers/blends are important for optimizing the processing conditions.<sup>47</sup> The rheological properties PP-R matrix are investigated using an in-line wedge rheometer. The shear thinning behaviors of the viscosity of neat PP-R are observed at different processing temperature (Fig. 6). It is note that the viscosity of PP-R melts decrease when increasing the processing temperature. Interestingly, at processing temperature higher than 200°C, PP-R melt presented similar viscosity at higher shear rate (ca. > 50 s<sup>-1</sup>). This behavior indicates we can achieve low viscosity of PP-R melt by increasing shear rate upto 50 s<sup>-1</sup> instead of by pushing up the processing temperature.

To elucidate the shear thinning behavior of PP-R at varied temperature, we conducted the rheological study at fixed shear rate (40 s<sup>-1</sup>). When plotting

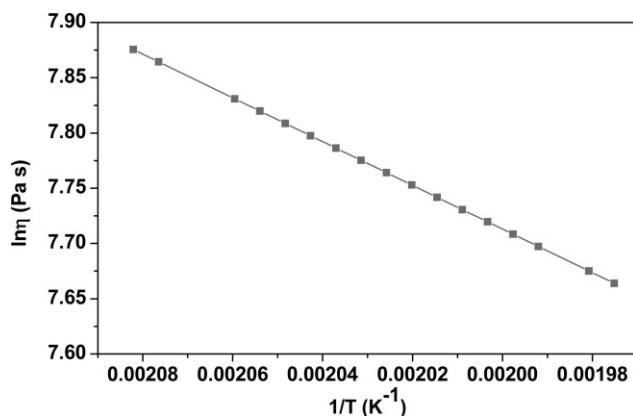


**Figure 7** Variation of melt viscosity of PP-R with temperature at fixed shear rate (40 s<sup>-1</sup>).

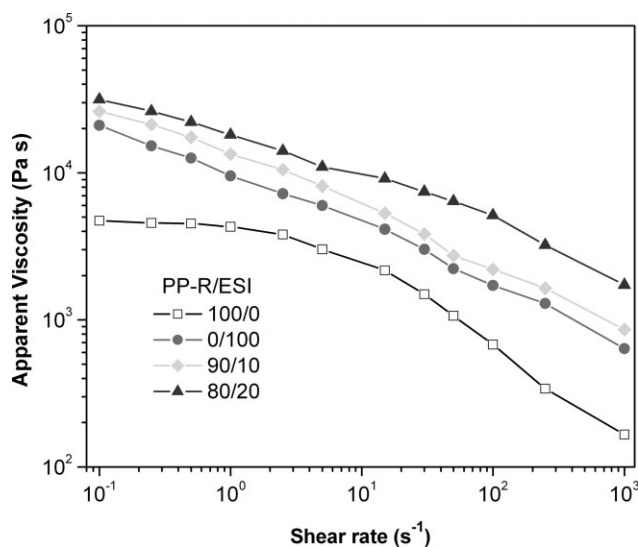


**Figure 8** Plots of apparent viscosity versus shear rate for PP-R/ESI blends.

logarithmic viscosity against  $1/T$  ( $K^{-1}$ ) (Fig. 7), a good linear relationship is obtained, this agrees well with the nonlinear relationship between  $\log \eta$  and  $1/T$  in Arrhenius equation,

$$\eta = A \cdot \exp^{\Delta E_{\eta}/RT}$$

where,  $\Delta E_{\eta}$  is the activation energy,  $R$  the gas constant, and  $A$  a materials constant. Taking the slope in Figure 7, the activation energy of PP-R is calculated to be 16.4 kJ/mol, which is only half of  $\Delta E_{\eta}$  values (37.5–41 kJ/mol) for the conventional PP.<sup>47</sup> This large difference in  $\Delta E_{\eta}$  can be explained by less regioregularity in PP-R polymer chains. Therefore, PP-R is less sensitive to temperature in comparison with PP during melt processing.

With the addition of ESI, PP-R/ESI blends exhibit higher viscosities than pure PP-R and ESI (Fig. 8). Importantly, ESI presented higher complex viscosity than PP-R matrix at all shear rates. The viscosity of the blends increases with the increment in ESI content in the blend. This viscosity enhancement may be explained by emulsion character of polymer blends in terms of effects of rheological properties of the blend components and concentration of the dispersed phase. As mentioned, ESI can push its rigid PS block to disperse well in PP matrix by use the affinity of its ethylene segments with PP-R matrix. The droplet-matrix morphology can be stabilized in the blend. As indicated from their MFI, PS blocks have higher viscosity than PP-R matrix. The emulsion effect at the interface increases with increasing ESI concentration. Consequently, the blends exhibit higher viscosities upon increasing ESI content ( $\leq 20$  wt %) than that of pure PP-R. On the other hand, disentanglements occur at the interface between PP-

R and ESI when increasing the shear rate. Therefore, the viscosity of blends decreased with increasing the shear rate, as shown in Figure 8.

## CONCLUSIONS

ESI is an effective impact modifier for PP-R and super-toughed polymer blends are achieved with low amount of ESI (ca. 5 wt %). PP-R/ESI blends exhibit significant enhancement in toughness and ductility, but slow decrease in stiffness such as tensile strength and elastic modulus with the addition of ESI. SEM observations reveal that the improved impact strength of PP-R/ESI blends is attributed to cavitation and shear yielding of matrix PP-R. Thermal analysis shows that ESI behaved as a nucleating agent for PP-R matrix.

The rheological measurements showed that PP-R matrix present shear thinning behaviors at shear rates regardless the processing temperature. At fixed shear rate, the nonlinear relationship between logarithmic viscosity against  $1/T$  agrees well with Arrhenius equation. For PP-R/ESI polymer blends. In comparison with conventional PP, PP-R is less sensitive to temperature during melt processing.

## References

- Kocsis, J. K. *Polypropylene Structure, Copolymer and Blends*; Chapman & Hall: London, 1995.
- Karian, H. G. *Handbook of Polypropylene and Polypropylene Composites*; Marcel Dekker: New York, 2003.
- Chiu, W. Y.; Fang, S. J. *J Appl Polym Sci* 1985, 30, 1473.
- Blom, H. P.; The, J. W.; Rudin, A. *J Appl Polym Sci* 1995, 58, 995.
- Kim, G. M.; Michler, G. H.; Gahleitner, M.; Fiebig, J. *J Appl Polym Sci* 1996, 60, 1391.
- Kotter, I.; Grellman, W.; Koch, T.; Seidler, S. *J Appl Polym Sci* 2006, 100, 3364.
- Choudhary, V.; Varma, H. S.; Varma, I. K. *Polymer* 1991, 32, 2534.
- Chen, C. Y.; Yunus, W. M. Z. W.; Chiu, H. W.; Kyu, T. *Polymer* 1997, 38, 4433.
- Van Der Wal, A.; Mulder, J. J.; Oderkerk, J.; Gaymans, R. J. *Polymer* 1998, 39, 6781.
- Van Der Wal, A.; Nijhof, R.; Gaymans, R. J. *Polymer* 1999, 40, 6031.
- Tasdemir, M.; Yildirim, H. *J Appl Polym Sci* 2002, 83, 2967.
- Liu, Y. Q.; Zhang, X. H.; Gao, H. M.; Huang, F.; Tan, B. H.; Wei, G.; Qiao, J. L. *Polymer* 2004, 45, 275.
- Val Der Wal, A.; Gaymans, R. J. *Polymer* 1999, 40, 6067.
- Mustafa, O.; Mehmet, E. *J Appl Polym Sci* 2005, 98, 1445.
- McNally, T.; Mcshane, P.; Nally, G. M.; Murphy, W. R.; Cook, M.; Miller, A. *Polymer* 2002, 43, 3785.
- Zhang, X.; Xie, F.; Pen, Z.; Zhang, Y.; Zhang, Y.; Zhou, W. *Eur Polym J* 2002, 38, 1.
- Lim, J. W.; Hassan, A.; Rahmat, A. R.; Wahit, M. U. *J Appl Polym Sci* 2006, 99, 3441.
- Da Silva, A. L. N.; Tavares, M. I. B.; Politano, D. P.; Coutinho, F. M. B.; Rocha, M. C. G. *J Appl Polym Sci* 1997, 66, 2005.
- Paul, D. R.; Bucknall, C. B. *Polymer Blends*; Wiley Interscience: New York, 2000.
- Pearson, R. A.; Sue, H. J.; Yee, A. F. *Toughening of Plastics*; American Chemical Society: Washington DC, 2000.

21. Wu, S. *Polymer* 1985, 26, 1855.
22. Wang, X.; Feng, W.; Li, H.; Ruckenstein, E. *Polymer* 2002, 43, 37.
23. Tjong, S. C.; Xu, S. A.; Mai, Y. W. *J Appl Polym Sci* 2003, 88, 1384.
24. Hisamatsu, T.; Nakano, S.; Adachi, T.; Ishikawa, M.; Iwakura, K. *Polymer* 2000, 41, 4803.
25. Mirabella, F. M. Jr., *Polymer* 1993, 34, 1729.
26. Hayashi, T.; Inoue, Y.; Chujo, R. *Macromolecules* 1988, 21, 3139.
27. Feng, Y.; Hay, J. N. *Polymer* 1998, 39, 6589.
28. Wang, D.; Gao, J. *J Appl Polym Sci* 1997, 99, 670.
29. Ebner, K. *Advances in Plastics Technology APT'96, International Conference*; Katowice, Poland, November 26–28, 1996; Paper 15, p. 1.
30. Zhao, M.; Gao, J. G.; Deng, K. L.; Zhao, X. Y. *New Materials of Modified Polypropylene*; Chemical Industry Press: Beijing, 2002.
31. Sterzynski, T.; Lambla, M.; Crozier, H.; Thomas, M. *Adv Polym Technol* 1994, 13, 25.
32. Abreu, F. O. M. S.; Forte, M. M. C.; Liberman, S. A. *J Appl Polym Sci* 2005, 95, 254.
33. Cheung, Y. W.; Guest, M. J. In *ANTEC '96 SPE Conference Proceedings*; Indianapolis, Indiana, 1996; Vol. 54, p 1634.
34. Chen, H.; Guest, M. J.; Chum, S.; Hiltner, A.; Baker, E. *J Appl Polym Sci* 1998, 70, 109.
35. Swogger, K. W.; Chun, S. P. In *MetCon '97 "Polymers in Transition" Conference Proceedings*; Houston, Texas, 1997.
36. Timmers, F. J.; The Dow Chemical Technology. U.S. Patent 5,703,187 (1997).
37. Chen, H. Y.; Stepanov, E. V.; Chum, S. P.; Hiltner, A.; Baer, E. *J Polym Sci Part B: Polym Phys* 1999, 37, 2373.
38. Chen, H. Y.; Stepanov, E. V.; Chum, S. P.; Hiltner, A.; Baer, E. *Macromolecules* 2000, 33, 8870.
39. Park, C. P. *J Polym Eng* 2001, 21, 511.
40. Tang, W. H.; Tang, J.; Yuan, H.; Jin, R. *J Polym Sci Part B: Polym Phys* 2007, 45, 2136.
41. Tang, J.; Tang, W. H.; Yuan, H.; Jin, R. *J Appl Polym Sci* 2007, 104, 4001.
42. Pabedinskas, A.; Cluett, W. R.; Blake, S. *Polym Eng Sci* 1991, 31, 365.
43. Yang, J.; Zhang, Y.; Zhang, Y. *Polymer* 2003, 44, 5047.
44. Willhelm, M. I.; Felisberti, M. I. *J Appl Polym Sci* 2002, 85, 847.
45. Yu, Z.-Z.; Yang, M.-S.; Dai, S.-C.; Mai, Y.-W. *J Appl Polym Sci* 2004, 93, 1462.
46. Setz, S.; Sticker, F.; Kressler, J.; Duschek, T.; Mulhaupt, R. *J Appl Polym Sci* 1996, 59, 1117.
47. Utracki, L. A. *J Rheol* 1991, 35, 1615.